

University Bremen

PMA Space Science and Technology M. Sc.

Project Report

Automated detection of Urban Heat Islands using remote sensing data

Linus Andrae (6015384)
October 10, 2023

Abstract

Urban Heat Islands (Urban Heat Islands (UHIs)) pose a growing health risk by exacerbating heat stress for residents of urban areas. Due to the increased prevalence of extreme weather events and heat waves and as a cause for higher energy consumption, UHIs become more relevant as a topic for city planners and policy makers to consider. Identification of areas most impacted or at risk require a data backed tool set to aid urban planning. This study presents a comprehensive pipeline developed using Python to automate the processing and analysis of Landsat 7,8 and 9 remote sensing imagery. The pipeline facilitates the generation of Normalized Difference Vegetation Index (NDVI) and heat maps, running statistical analysis of factors known to create UHIs of a provided area of interest, serving as a robust toolset for the investigation and detection of UHIs. The methodology employed leverages the spectral characteristics of Landsat data to provide high-resolution insights into temperature variations within urban areas as well as statistical analysis of the composition of the identified Urban Heat Islands. The ultimate aim is to offer actionable guidance to city planners and developers for the mitigation of UHIs, by classification of UHIs on different scales. At the current implementation level the pipeline is able to detect UHIs from level one brightness temperature and the statistical analysis indicate a strong correlation between land cover types and heat island intensity, affirming the utility of the pipeline in urban climate studies.

Contents

1	Introduction	4
2	Background	4
2.1	Urban Heat Islands	4
2.2	Land Surface Temperature	4
2.3	Normalized Differential Vegetation Index (NDVI)	4
2.3.1	NDVI Colormap	5
3	Objectives	7
4	Scope	7
5	Methodology	7
5.1	Data Quality	7
6	Implementation	8
6.1	Pipeline design	8
6.2	Loading an Image	8
6.3	Preprocessing	8
6.4	Land Surface Temperature Calculation	8
6.4.1	Calculation of the Landsat L2 LST	8
6.4.2	Estimation of the LST temperature based on Landsat L1 Data	8
6.5	Surface classification	9
6.6	Detection of the Urban Heat Islands	9
6.7	Further analysis steps (not yet implemented)	10
7	Analysis	12
7.1	Comparison of Top of Atmosphere (TOA) and L2 Land Surface Temperature (LST)	12
7.2	UHI detection	13
8	Results	14
9	Discussion	16
10	Conclusions and Outlook	16

List of Figures

1	Absorption spectrum of green vegetation[3, Fig. 2]	5
2	NDVI Images from the different satellites	5
3	Different color maps used show the better ability to differentiate between green vegetation and desert and buildings within Phoenix	6
4	Pipeline stages for data processing	8
5	Classification of the Bremen Land usage using K-Means	10
6	UHIs detected in Karlsruhe based on L1 and L2 Data	11
7	UHIs detected in Speyer based on L1 and L2 Data	11
8	UHIs detected in Bremen based on L1 and L2 Data	11
9	Difference between L1 and L2 Data of Bremen	12
10	Correlation between the observed TOA and the L2 LST	12
11	Land Surface Temperature versus NDVI value	13
12	Results of the clustering and histograms on channel	14
13	LST and NDVI values of the pixels within the classes on a pixel based level	15

List of Tables

1	The mapping of OSM Tags and KMeans surface classification types	9
2	Temperatures and UHIs observed in different Cities	14

Acronyms

USGS United States Geological Survey

LST Land Surface Temperature

LULC Land Use/ Land Cover

UHI Urban Heat Island

NDVI Normalized Differential Vegetation Index

NIR Near Infrared

OSM Open Street Map

TOA Top of Atmosphere

1 Introduction

Investigation on Urban Heat Islands (UHIs) using remote sensing data is a widely used technique to investigate surface temperature UHIs. To investigate statistical relations between surface types, land surface temperature and vegetation, a software product was developed that processes multispectral remote sensing data of Landsat 7, 8 and 9 missions, to analyse the UHIs. This report is covering the theoretical background, development and function of the software, initial analysis on selected cities and an outlook how the software could be used for future analysis. This report covers the work done over the course of the summer semester as part of the Master Project module in cooperation with OHB Digital GmbH.

2 Background

2.1 Urban Heat Islands

The phenomenon of UHIs has been studied for the past 30 years. Due to increase in global temperature as well as increased occurrence of extreme weather and periods of heatwaves, this phenomenon will likely increase in intensity and will also occur in cities at higher latitudes [12][23, p. 904]. UHIs are a spacial phenomenon that occurs on different scales and intensities, this makes observation using remote sensing data a good and widely used approach [21].

UHIs are distinguished into surface and atmospheric UHIs. Within this context we will only investigate surface UHIs. Surface UHIs are areas of higher surface temperatures within urban areas compared to rural areas due to the materials used and heat from mobility, electrical appliances, heating and cooling as well as less vegetation and higher sealed surfaces that reduce surface water availability[17, pp. 7-12]. The surface UHIs are longer term phenomenon that are most intense in summer. Atmospheric UHIs are more dependent on weather and local topology and are in part a side effect of the slower cooling of the city air due to the higher thermal capacity and wind obstruction. This phenomenon is not investigated by this work, since the air temperature can not be directly observed by remote sensing data. The main factors in forming urban heat islands is the thermal storage capacity of materials used in urban areas like concrete, asphalt and steel, that have a high heat capacity and heat up quickly during the day and emit the stored thermal energy as sensible heat with a delay (eg. during the night)[11]. High surface sealing and lack of vegetation reduce surface water availability and diminish evaporation and the cooling effect of latent heat causing more thermal energy to be available as sensible heat. Another factor is the heat produced by human activity such as industrial processes and combustion engines. As a consequence of higher temperatures, active cooling devices are more frequently used for buildings and vehicles. The emitted thermal energy of these heat pumps further increases the surrounding temperature, reinforcing the effect.

There are multiple adverse effects and possible mitigation techniques for the mitigation and reduction of urban heat islands have been studied extensively since the 1970s[9][16]. Advective cooling can be observed when the temperature gradient generated airflow from the cooler surrounding areas towards the hot areas within the city, cooling it down[4].

Urban areas with no close water body (generating sea breezes as well as latent heat transport) and with lower average wind speed are more likely to be affected by urban heat islands[10]. Higher temperatures due to UHIs cause stress to animals and humans increasing health risk due to heat stroke and increased surface level ozone concentration[13].

2.2 Land Surface Temperature

Land surface temperature is the temperature at which an object emits infrared radiation according to plank's law[6]. Using remote sensing methods this quantity can not be directly observed since the satellite is observing TOA brightness temperature. This temperature can be transformed to a LST using atmospheric correction and correction for the emissivity of the ground. The conversion factor is data source dependent and can be found in Section 6.4.2.

2.3 Normalized Differential Vegetation Index (NDVI)

The Normalized Differential Vegetation Index (NDVI) is an widely used index using the difference of the red and near infrared bands to determine the amount of green vegetation.

$$NDVI = \frac{Red - NIR}{Red + NIR} \quad (1)$$

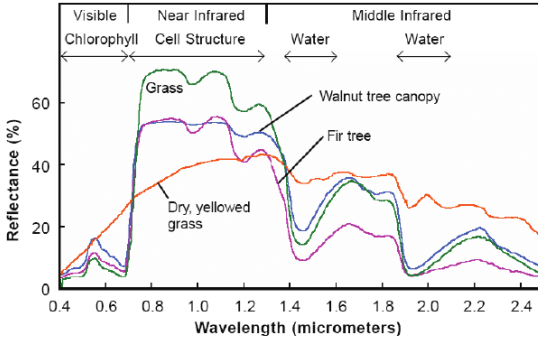
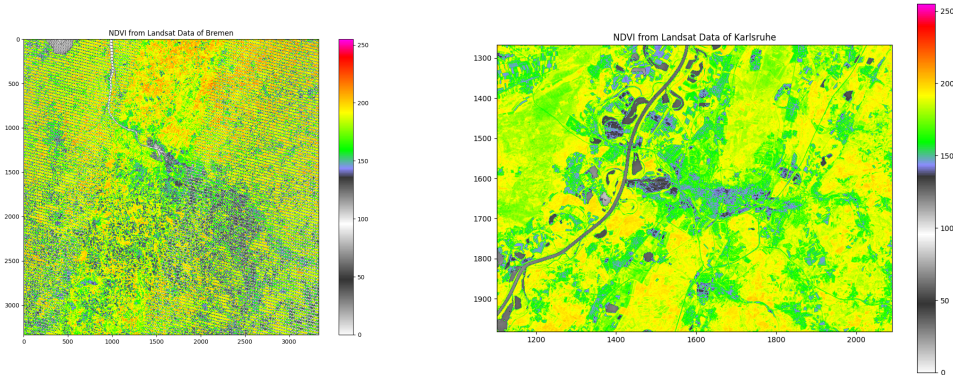


Figure 1: Absorption spectrum of green vegetation[3, Fig. 2]

For Landsat 7 data channel 3 (red and orange: 630 nm – 690nm) and channel 4 (near infrared 780 nm–900nm) are used for NDVI calculation. For Landsat 8 and 9 data, channel 4 (red 640 nm – 670 nm) and channel 5 (near infrared 850 nm – 880 nm) where used. As shown in Fig. 1 healthy plants reflect near infrared and there is a sharp rise in reflectance between the two used channels at around 700 nm. This index is used for emissivity estimation for Land Surface Temperature calculation see Eq. (2), correlation with heat islands (since there is a negative correlation between those two values, due to the latent heat of evaporation reducing surface temperature at higher vegetation areas).

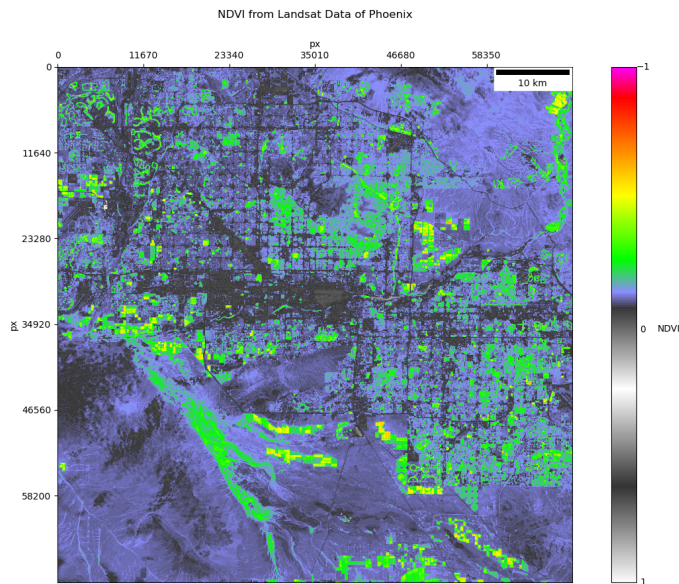


(a) NDVI of Bremen (Bands 5 and 6) using Landsat 7 data on 2019-07-23 (b) NDVI of Karlsruhe (Bands 4 and 5) using Landsat 8 data on 2023-06-07

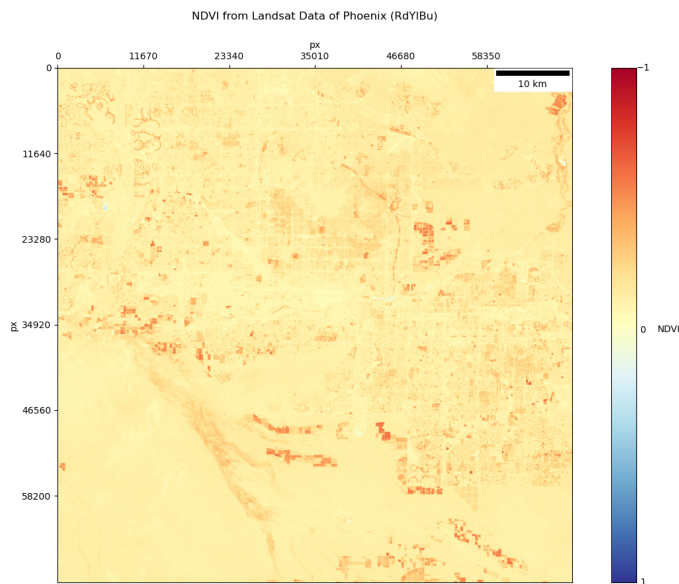
Figure 2: NDVI Images from the different satellites

2.3.1 NDVI Colormap

When using a classical heat map with a color gradient from colder to warmer colors or a diverging color map (see Fig. 3b), details of the image get lost and it is hard to distinguish plant health, build up and vegetated areas and the difference between small NDVI changes. To aid an intuitive understanding a specially created colormap can be used. The color map was adapted for use in python from work of public lab[8] where it was developed in an attempt to create color-blind friendly NDVI color maps. Values below 0.2 are areas with no vegetation. The color map used in Fig. 3a uses a gradient of gray with a “black-white-black white” transition to allow higher dynamic range for non vegetation areas. For areas with an $\text{NDVI} < 0.2$ blue is used. Green values are low or unhealthy green vegetation or mixed use pixels. Orange and red values correspond to thicker vegetation e.g. forests, parks or green fields. Comparing Fig. 3a and Fig. 3b where most of the desert surrounding the city has no green vegetation and the parts covered in vegetation can be clearly distinguished from the arid desert regions. Still the surface roughness can be seen quite well due to the gray scale gradient in the < 0.2 NDVI range.



(a) NDVI Image of Phoenix with the VGYRM color map



(b) NDVI Image of Phoenix with a RdYIbu gradient color map

Figure 3: Different color maps used show the better ability to differentiate between green vegetation and desert and buildings within Phoenix

3 Objectives

The goal of the project was to investigate UHIs using remote sensing data. To find out what steps are needed to detect UHIs in different climate and seasonal conditions multiple cities where investigated. The cities where investigated in different time frames and different data sources where used. The cities that where selected where:

- Bremen due to the possibility to locally verify land use on ground
- Karlsruhe, this city developed a heat action plan and has an interesting geology
- Speyer lies in one of the hottest areas in Germany with more than 40 days per year with over 25 °C that is in a similar geographical area as Karlsruhe and allows comparison of urban and geographic features due to close distance between cities

Other questions that this work wanted to answer where:

- How strong is the correlation between UHIs and vegetation?
- Can a simple estimation of the land surface temperature be enough to detect UHIs compared to the Level two products of the satellite data.

4 Scope

Part of this effort was the planning, development and verification of software that UHIs can be detected using remote sensing data automatically. The data processing of the pipeline that was developed was verified and statistical analysis about land usage, vegetation and temperature data where conducted. The developed software is used as parts of the toolset for further analysis of UHIs as part of a master thesis.

5 Methodology

The process used in this project used a data driven approach to answer the questions above. First the available remote sensing data sources where evaluated and the Landsat satellites where selected due to availability, usage in similar research towards UHIs[22][21][5] where selected. Based on the possibilities to do local on site verification Bremen was chosen as a first area of investigation. From the remote sensing data the NDVI and LST where calculated and surface type classification was done. Based on the derived data statistical analysis where made to investigate the correlation between NDVI, surface types and LST. The same approach was done for Landsat 7 and Landsat 8 images. Urban heat islands where detected using statistical analysis of the derived LST data.

5.1 Data Quality

The Landsat 7 Data has a resolution of 30m x 30m for all channels but the thermal channels, the thermal infrared channels have 60m x 60m per pixel[18] with 8 bit color depth. In Landsat 7 Images only scenes can be properly used where the targeted area of interest lies in the center region of the swath, since starting in march 2003 the scan line correction onboard the ETM+ instrument failed and up to 22% of the scene can not be used[18]. For Landsat 8 Data the resolution of the reflective channels are identical, the thermal channels have a 100m x 100m resolution with a higher grayscale color range per pixel of 12-bit[19]. Errors due to cloud shadows[2, p.14] where eliminated by using images with no clouds for the areas of interest.

6 Implementation

The application that was created uses python and the luigi module to allow building scalable pipelines with automated dependency management. This allows to change a single stage in the pipeline and allow automatic inclusion of switched dependencies or additional process steps that can be configured by passing parameters to prior steps within the pipeline. To allow quick adaption and partly automated analysis different software modules were created. This part will give an overview over the implemented parts, the overall workings and outlook for possible additions and shortcomings of the currently implemented software.

6.1 Pipeline design

The python software is designed as a data pipeline with different steps that automatically trigger previous requirements when run using the Luigi module[7]. A startup script initiates the pipeline by calling the last stage as a luigi task. Each tasks will in turn start the required previous stages it depends on for execution, building up a requirement graph that will start the end nodes once all requirements where found. Once a stage or task is completed the next step is triggered and run. In case of an error the pipeline execution will be stopped. Figure 4 shows the software data flow, purple steps are part of the UHI detection and statistical analysis and purely based on Landsat data. Blue steps are related to Land Use/ Land Cover (LULC) classification. Yellow steps are future additions and not implemented yet. In the following section each pipeline stage will explained for the steps in turquoise and purple shown in Fig. 4.

6.2 Loading an Image

The images in GEOTIFF format can be loaded by the pipeline as single bands (LoadBands, LoadNDVIBands) or as a full set of Bands (LoadFullLandsatDataToXarray). Bands are loaded as numpy arrays and in the full set load function stored inside an xarray data structure where each band data is named individually by band name, to ease usage independent of the data source band enumeration. Between pipeline steps the data is stored in a temporary zipped numpy binary format npz, this allows multiple steps to work with the same output.

6.3 Preprocessing

The preprocessing of the images is done by cropping the image to the area of interest by providing a center coordinate and the bounding box height and width in m (north-south and east-west sizes) The transformed image might be filtered if needed by a later pipeline stage.

6.4 Land Surface Temperature Calculation

6.4.1 Calculation of the Landsat L2 LST

The United States Geological Survey (USGS) provides LST data for Landsat 7,8 and 9 Thermal instruments[2][1] online after around two weeks after data acquisition. The level two data set uses the top of the atmosphere temperature and calculates the LST using atmospheric correction, correction for absorption and emissivity based on ASTER GED data set for radiation temperature.

6.4.2 Estimation of the LST temperature based on Landsat L1 Data

To check the functionality of the pipeline and create a possibility to create land surface temperature maps from raw data a estimation algorithm was implemented based on the Landsat level 1 data. It was correction for emissivity based on the NDVI, this is not as accurate as the ASTER data but

provides LST maps quickly and can be derived from a single image data set of the Landsat mission. The landsat intensity value can be converted to a brightness temperature using Eq. (2)(see [20])

$$L_\lambda = M_L \cdot Q_{cal} + A_L$$

$$BT_{TOA} = \frac{K2}{\ln(\frac{K1}{L_\lambda} + 1)} \quad (2)$$

For the L_λ the TOA radiance is calculated from the M_L parameter from the band meta data file and the additive rescaling factor that is also included in the meta data of the image. Where K1 and K2 are satellite dependent correction parameters and L_λ is the observed brightness temperature at the satellite instrument. The resulting TOA brightness temperature is then corrected using fixed factors based on the NDVI. The conversion to LST can be done using satellite dependent steps and the correction based on NDVI are for Landsat 8 and for Landsat 7.

$$LST = \frac{T_{TOA}}{1 + \frac{\epsilon \cdot T_{TOA}}{1.4388}} \quad (3)$$

To approximate a proper emissivity correction the Eq. (4)[15] is used.

$$\epsilon = m \cdot P_v + n$$

$$P_v = \frac{NDVI - NDVI_{min}}{NDVI_{max} - NDVI_{min}} \quad (4)$$

With P_v beeing the vegetative fraction where n and m are correction factor for emissivity of partly vegetated areas. For NDVI values below 0.2 the surface is assumed to be not populated by any green vegetation and the emissivity is taken from the red band[9]. For $NDVI > 0.5$ the area of a pixel is assumed to be fully vegetation and the emmissivity can be assumed as 99%[15] and the values in between can be calculated by the above method with m and n taken from previous research as $m = 0.004$ and $n = 0.986$ [15, equ. 12a&b]. In the following analysis the BT_{TOA} is used without emissivity correction, to test and show that the raw data can be used to detect UHIs.

6.5 Surface classification

As basis for the statistical analysis and to classify the composition and formation of UHIs LULC must be determined and differentiated, this was done using k-means as a pixel based clustering algorithm. The classification algorithm used blue, green, red and near infrared bands of the datasets to find pixel that have a similar composition. By referencing the against Open Street Map (OSM) land classification dataand local on site verification the classification results where verified. An automatic pixel based comparison did not yield the desired results so a manual verification was done using the above mentioned resources. For future usage it would be suggested to use Sentinel-2 land cover or any other high resolution LULC data set for verification. For the OSM verification the land usage types shown in Table 1 of OSM where used af the HeiGIT OSMLandUseLandCover project where used for manual verification (see Fig. 5)

K-Means Classification	OSM tag
Low density residential streets	residential, commercial, religious, education, recreation_ground
Residential low vegetation	residential, commercial, religious, education
Industry	construction, industrial, depot, port, railway, garages
Industry Halls	industrial, depot
Vegetation Agriculture	farmland, meadows
Fields Meadows	farmland, meadows, grass, recreation_ground
Forests, trees & dense vegetation	cemetery, trees, forest
Water	water
No Data	—

Table 1: The mapping of OSM Tags and KMeans surface classification types

6.6 Detection of the Urban Heat Islands

To detect the UHIs from the LST calculated before, a simple statistical threshold was applied. The temperature has to be by more then 2.5σ higher then the average temperature of the image

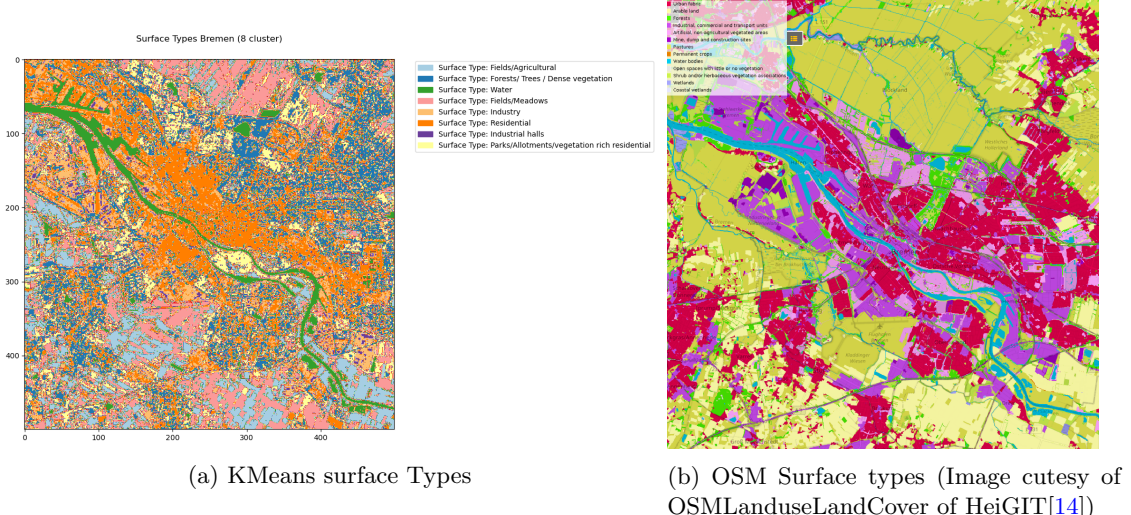
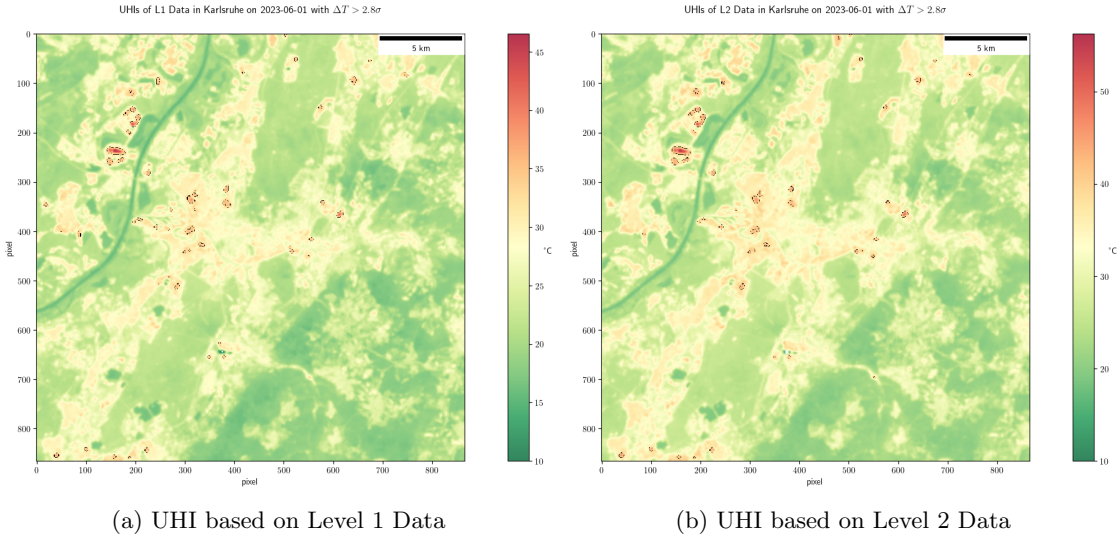


Figure 5: Classification of the Bremen Land usage using K-Means

section, to be classified as a UHI. The threshold of 2.8 was used to make results more comparable between cities. The usage of the mean of the whole area might cause a lower mean temperature if the shape of the urban area is ellipsoidal and surrounded by colder surfaces, this could be mitigated by either using a shape file to limit the area used for calculation or changing the threshold value for UHI detection. Since city limits do not correspond to an immediate change in LULC this was not done in the cities investigated here. The LST image where post processed to find all high heat areas and find and label connected high heat pixels to create contours of the significant higher temperature regions (shown in Fig. 6, Fig. 7 and Fig. 8). Areas smaller then 3 pixels were filtered out, since these likely correspond to single high heat or reflectivity pixels due to single roofs or other buildings, that did not cause a heating effect over a larger area. /newpage

6.7 Further analysis steps (not yet implemented)

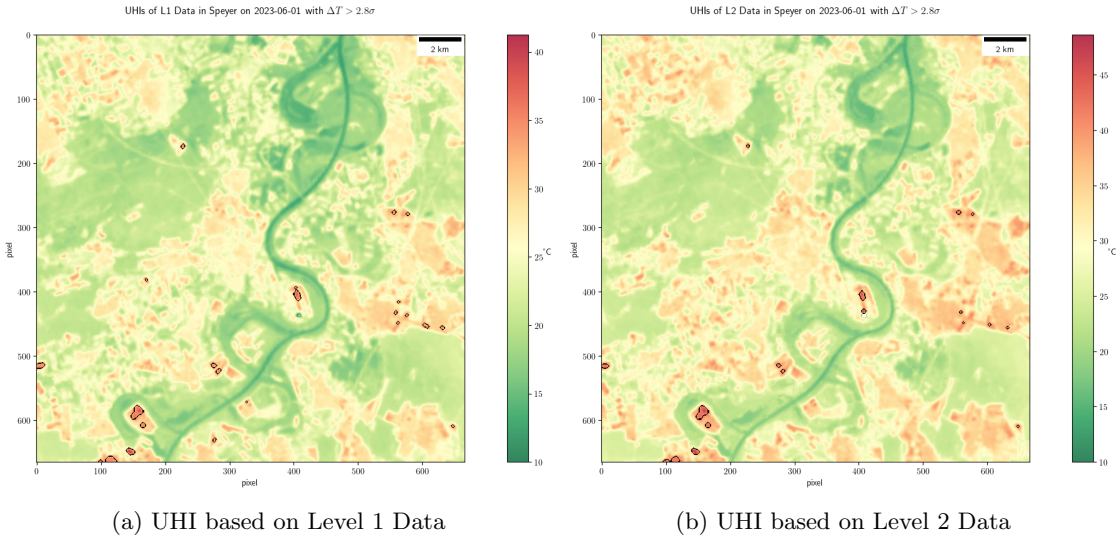
After UHIs where detected further analysis could be added to the pipeline. A watershed analysis of the UHIs can be used to dynamically vary the threshold what areas are affected by the UHI from each center pixel to analyse scale effects of the UHIs. Another possible addition would be to analyse the shape of the UHI contour with different thresholds or at different seasons to investigate the influence of mean temperature, seasonal changes, city development and rising mean temperatures over time due to climate change on the UHI effect.



(a) UHI based on Level 1 Data

(b) UHI based on Level 2 Data

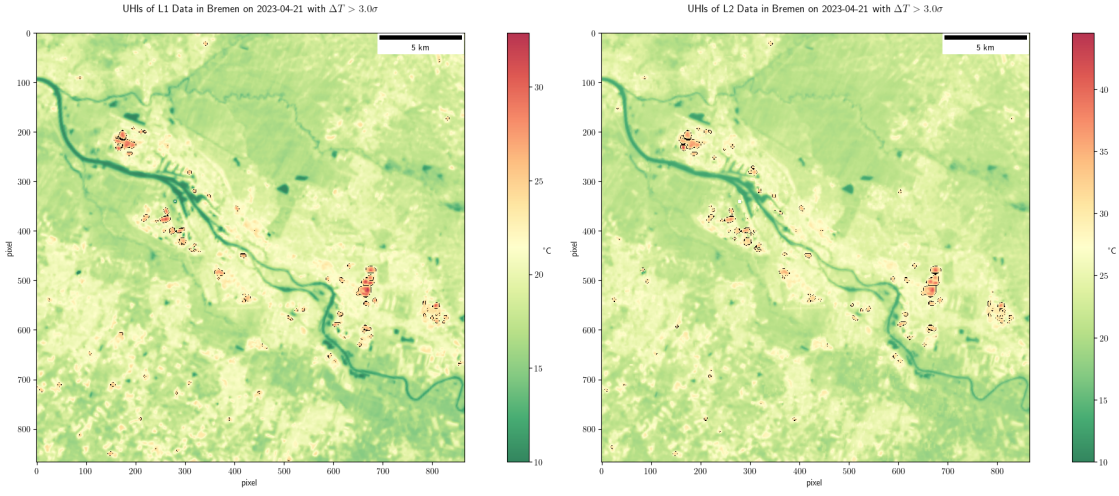
Figure 6: UHIs detected in Karlsruhe based on L1 and L2 Data



(a) UHI based on Level 1 Data

(b) UHI based on Level 2 Data

Figure 7: UHIs detected in Speyer based on L1 and L2 Data



(a) UHI based on Level 1 Data

(b) UHI based on Level 2 Data

Figure 8: UHIs detected in Bremen based on L1 and L2 Data

7 Analysis

7.1 Comparison of TOA and L2 LST

Comparing the two data sets, a significant offset was seen between the L2 LST and the TOA from the L1 data (see Fig. 9). The range of temperatures was more than 50% bigger in the data that was not corrected for emissivity compared to the L2 data corrected by the USGS using the ASTER emissivity database. This suggests that emissivity correction is needed for high quality result when working with absolute temperatures. The uncorrected data does allow basic detection of UHI since the relative temperatures are spread out more but the internal distribution doesn't change significantly (see the high correlation between the offset temperature data in Fig. 10a – Fig. 10c).

This allows the detection of UHIs based on level one data, while taking some under detection into account, due to atmospheric dampening. This allows to use Landsat L1 data for creating relative temperature maps that are able to detect urban heat island, since the UHI is a relative temperature effect. For level two data an uncertainty value is given for each pixel. For the

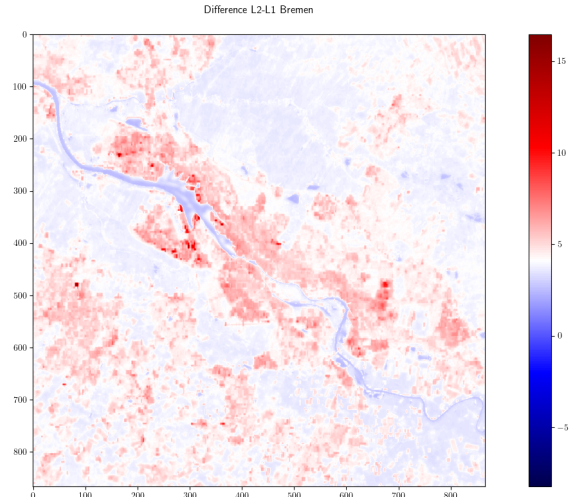


Figure 9: Difference between L1 and L2 Data of Bremen

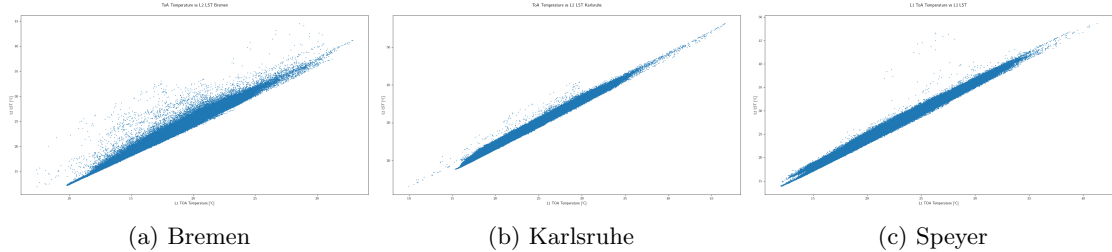


Figure 10: Correlation between the observed TOA and the L2 LST

Bremen image with a range of 1.8 ° to 9.5 °C with an RMS error of 2.62 °C, the whole temperature range was offset compared to the L1 data to higher temperatures (by 5.37 °C on average). There where 41 pixels in three clusters with very high uncertainty values (above 7 °C), these where all located over industrialized areas and are likely caused by smoke plumes or the reflections of industry hall roofs. For Karlsruhe the maximum uncertainty for level two data was 7.98 °C the minimum 1.93 °C and the RMS uncertainty was 2.5 °C. All 18 pixels with more then 7 °C uncertainty where located in two clusters over industrial areas. For Speyer the maximum uncertainty for level two data was 6.11 °C the minimum 1.99 °C and the RMS uncertainty was 2.7 °C. The highest degree of uncertainty was observed over the water surfaces, specifically over the river Rhine.

7.2 UHI detection

Using Landsat 7 and Landsat 8 data it was possible to identify urban heat islands in Bremen, Karlsruhe and Speyer using the level 1 and level 2 data products shown in Fig. 6, Fig. 7 and Fig. 8. A statistical analysis was done on the correlation between the LST and the different land cover types as well as the NDVI and the LST. The following data used the Landsat 8 Acquisition of Bremen from 2023-04-21 and the level 2 LST data was used. In Fig. 11 the LST of each pixel is shown with the corresponding NDVI value and the class for each pixel. The Water pixels had a low NDVI as to be expected and had the lowest temperatures within the image. It can be seen that

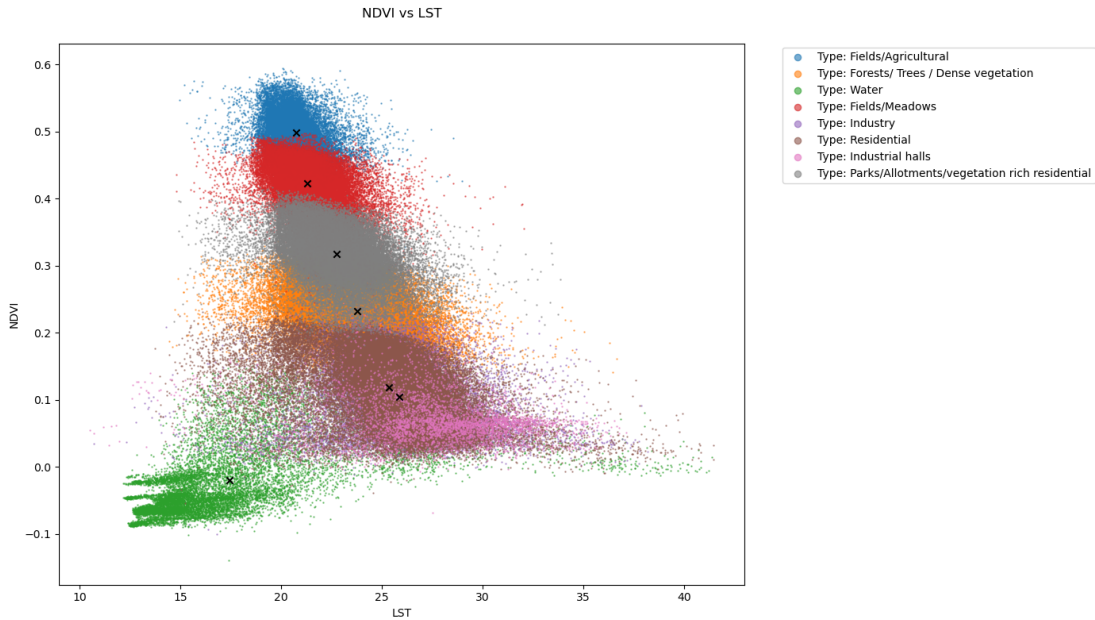


Figure 11: Land Surface Temperature versus NDVI value

there is a strong correlation for all clusters except the water class between low temperatures and a high NDVI and higher temperatures and low NDVI. The classes that were created using the kmeans algorithm and four bands show the distinction of classes in the amount of vegetation that is found within the pixels of each type in Fig. 13b and for the distribution of LST for each class in Fig. 12. As seen in the scatter plot (Fig. 13) the clusters were mainly distributed within the near infrared band since the other bands have a very high correlation (> 0.95 in the investigated images). Since this channel is used for NDVI creation, there is a high correlation between NDVI and classification. It can be seen that the highest brightness values are part of the industry halls that contains all metal roofed large buildings that reflect in all wavelengths. The other clusters are mainly distributed along the Near Infrared (NIR) intensity values and then differ slightly within colors (e.g. green intensity for different vegetation classes while the center of built up classes differ within the blue or red intensity). The LST distribution between classes shows small dense clusters of temperatures near the mean temperature for all vegetation classes with low growing vegetation having the lowest spread of temperature. Built up land classes have a high temperature spread and higher mean and median temperatures. The 0°C temperature value for the *Industry halls* class is caused by four pixels with no data due to invalid data in the LST dataset. The very high spread temperature within the water class is in part explained by the temperature anomalies mentioned earlier and on the other hand by the different types of water bodies found within the image (small lakes, ditches and ponds as well as the river Weser).

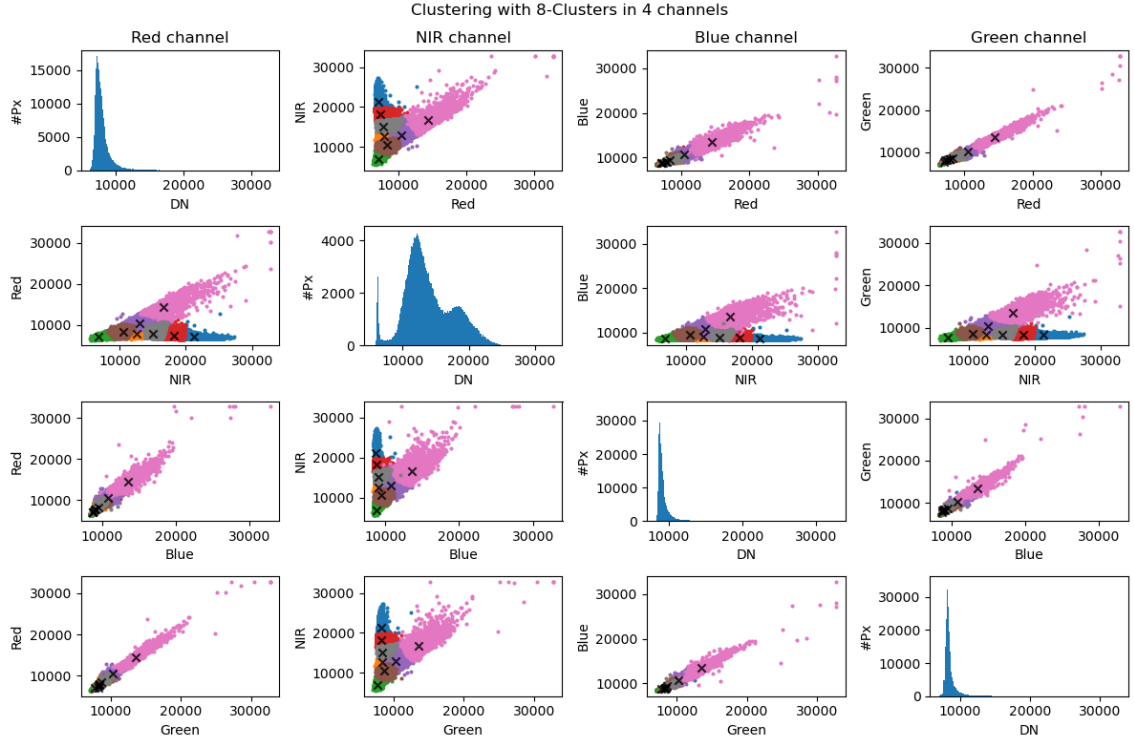


Figure 12: Results of the clustering and histograms on channel

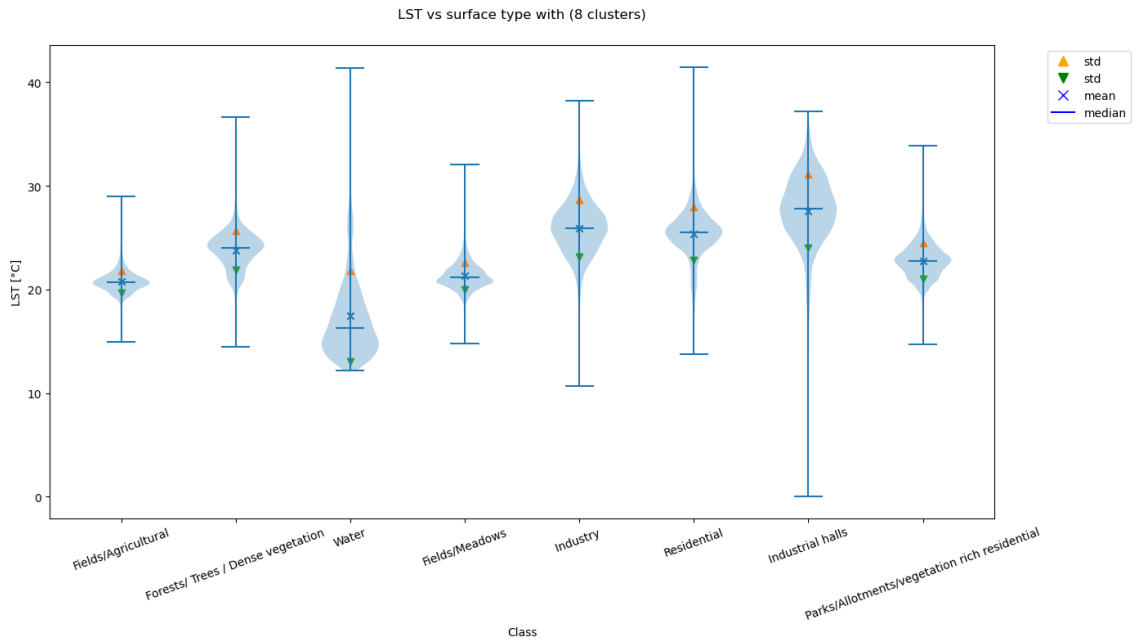
8 Results

Using the Landsat satellite data allowed the calculation of the LST for all investigated areas without emissivity correction with an offset of between 2 and 12 °C on average for the three investigated areas. The level two correction for surface material emissivity does change the surface temperature values but not significantly change the temperature distribution. The average temperature of the selected areas and the maximum temperatures detected in the UHIs are shown in Table 2. The

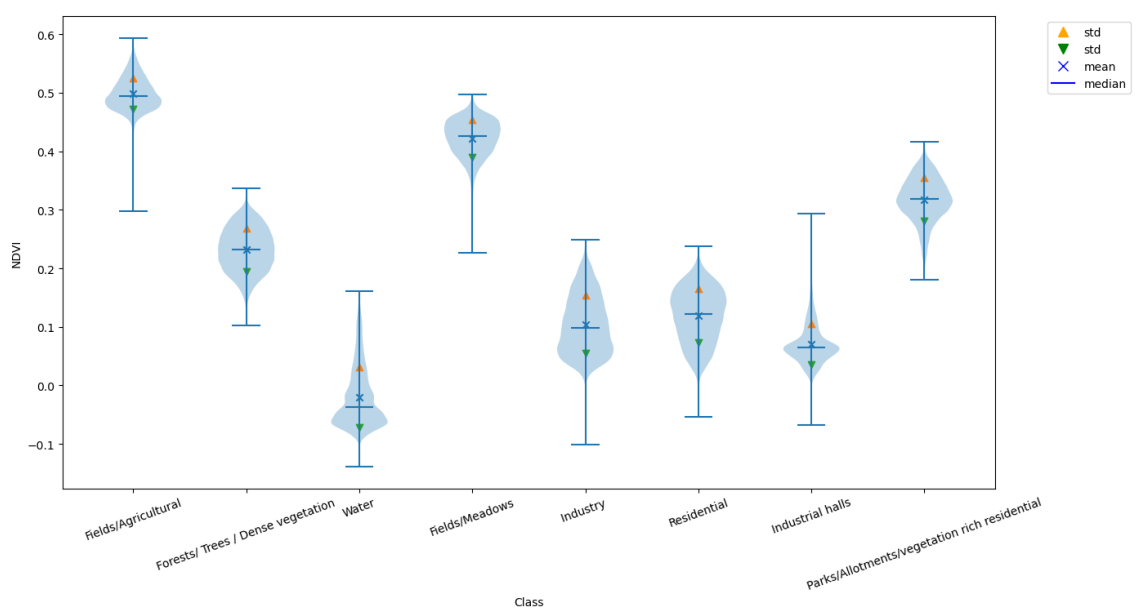
City	Mean LST	LST_{min} [° C]	LST_{max} [° C]	#UHIs (threas.)
Bremen L1 (2023-04-21)	18.38 ($\sigma = 2.05$)	6.6	32.87	70 (3 σ)
Bremen L2 (2023-04-21)	22.68 ($\sigma = 2.62$)	12.0	44.54	84(3 σ)
Karlsruhe L1 (2023-06-01)	23.48 ($\sigma = 3.83$)	9.32	46.54	86 (2.5 σ)
Karlsruhe L2 (2023-06-01)	27.91 ($\sigma = 4.81$)	13.15	56.25	74 (2.5 σ)
Speyer L1 (2023-06-01)	22.94 ($\sigma = 3.88$)	9.34	41.26	49 (2.5 σ)
Speyer L2 (2023-06-01)	27.47 ($\sigma = 4.87$)	13.8	48.64	39 (2.5 σ)

Table 2: Temperatures and UHIs observed in different Cities

statistical analysis was adapted for each city and can not be compared since the data was taken on different dates, the area of interest and shape of the cities are quite different and thus the mean temperatures and absolute thresholds are different. Comparing Karlsruhe and Speyer that have the same data set as baseline (both are within the same image captured on the same day by the Landsat 8 satellite). It can be seen that there are more UHIs detected in Karlsruhe (the city is bigger and the selected Area of interest is as well) then in Speyer. The mean and Also the Karlsruhe area has a higher mean temperature and higher maximum temperature. In both cities the heat islands were located within industrial areas, low temperatures where within vegetated or near water areas. Figure 8 shows Bremen at the end of april where the local air temperature of that day was at around 19 °C (Source: Deutscher Wetterdienst Bremen airport station) at the time of recording. The biggest heat islands detected within the area are all located within industrialized parts of the city.



(a) Surface temperatures of the pixels within each class, with minimum maximum and internal distribution



(b) NDVI values of the pixels within each class

Figure 13: LST and NDVI values of the pixels within the classes on a pixel based level

9 Discussion

The pipeline approach works quite well with different data sources and areas, to gain insides and analysis data quickly. The use of level 1 data to find UHIs based on temperature differentials allows to analyse real time data from the satellites that is less than a week old, while the level 2 LST is made available a few weeks after the acquisition. The extend of the detected UHIs varied between the processing levels while the affected areas remained the same. The processing steps should be improve to allow a higher similarity between the data levels, preprocessing of the data could eradicate outliers observed in the data sets (e.g. the zero value in the industry hall class in Fig. 11). Another verification approach should be implemented to verify the classification e.g. the Sentinel-2 land cover data. For further analysis especially when comparing cities a way must be found to define the UHIs by another metric then the mean temperature of the picture since the shape and urban composition as well as area selection influences the UHI detection. This can be optimized by not only take the statistical average temperature of the image as baseline but include the surface type classification to include only the temperature of the urban areas.

10 Conclusions and Outlook

Urban planning is tasked in the coming decades with increasing the mitigation and resilience of heat effects, increased flood risk due to extreme weather and other climate change related effects on cities. This requires a deep understanding and investigation of the underling phenomenons. Out of these insights technical and policy decisions need to be made, to protects inhabitants from the negative effects of the changing conditions.

Many of the possible solutions against one effect have an positive effect on other climate related urban phenomenons. Floodplains or natural wet vegetated areas within a city reduce temperature due to latent heat conversion and flood resistance due to higher water storage capacity of the city area and reduction of water ways. Trees reduce temperature and slow airflow within long and narrow streets.

In many cases only a few options are possible to implement due to geographic factors, construction area or budget limitations. To choose the most effective solutions the impact of possible options have to be known and compared. The development of tools, to allow quick analysis and measure the impact of implemented decisions, is one the steps in the needed courses of action. Remote sensing data, is an available, low cost and quick way to get an overview and possible areas to implement countermeasures. The implemented pipeline with python allows the use of two current and past earth observation satellite systems (Landsat 8 and Landsat 7) to analyse the current and past development of UHIs, aid decisions and judge the impact of implemented counter measures. While the implemented solution proposed in this far from feature complete it could serve as the base for further research and development as part of a tool set for scientists, policy makers and urban planners.

References

- [1] Earth Resources Observation And Science (EROS) Center. *Collection-2 Landsat 7 Enhanced Thematic Mapper Plus (ETM+) Level-2 Science Products*. 1999. DOI: [10.5066/P9C7I13B](https://doi.org/10.5066/P9C7I13B).
- [2] Earth Resources Observation And Science (EROS) Center. *Collection-2 Landsat 8-9 OLI (Operational Land Imager) and TIRS (Thermal Infrared Sensor) Level-2 Science Products*. Type: dataset. 2013. DOI: [10.5066/P90GBGM6](https://doi.org/10.5066/P90GBGM6). URL: <https://www.usgs.gov/centers/eros/science/usgs-eros-archive-landsat-archives-landsat-8-9-olitirs-collection-2-level-2> (visited on 09/16/2023).
- [3] M. Govender, K. Chetty, and H. Bulcock. “A review of hyperspectral remote sensing and its application in vegetation and water resource studies”. en. In: *Water SA* 33.2 (2007). ISSN: 1816-7950. DOI: [10.4314/wsa.v33i2.49049](https://doi.org/10.4314/wsa.v33i2.49049). URL: <https://www.ajol.info/index.php/wsa/article/view/49049> (visited on 09/03/2023).
- [4] Marie Haeger-Eugensson and Björn Holmer. “Advection caused by the urban heat island circulation as a regulating factor on the nocturnal urban heat island”. en. In: *International Journal of Climatology* 19.9 (1999), pp. 975–988. ISSN: 1097-0088. DOI: [10.1002/\(SICI\)1097-0088\(199907\)19:9<975::AID-JOC399>3.0.CO;2-J](https://doi.org/10.1002/(SICI)1097-0088(199907)19:9<975::AID-JOC399>3.0.CO;2-J). URL: <https://onlinelibrary.wiley.com/doi/abs/10.1002/%28SICI%291097-0088%28199907%2919%3A9%3C975%3A%3AAID-JOC399%3E3.0.CO%3B2-J> (visited on 09/10/2023).
- [5] Nasrin Adlin Syahirah Kasniza Jumari et al. “Analysis of urban heat islands with landsat satellite images and GIS in Kuala Lumpur Metropolitan City”. In: *Heliyon* 9.8 (Aug. 2023), e18424. DOI: [10.1016/j.heliyon.2023.e18424](https://doi.org/10.1016/j.heliyon.2023.e18424).
- [6] “Chapter 7 - Land surface temperature and thermal infrared emissivity”. In: ed. by Shunlin Liang and Jindi Wang. Academic Press, Jan. 2020, pp. 251–295. ISBN: 9780128158265. DOI: [10.1016/B978-0-12-815826-5.00007-6](https://doi.org/10.1016/B978-0-12-815826-5.00007-6). URL: <https://www.sciencedirect.com/science/article/pii/B9780128158265000076> (visited on 09/19/2023).
- [7] *Luigi Python Repository*. URL: <https://github.com/spotify/luigi>.
- [8] *New NDVI Colormap*. Online. Aug. 2014. URL: <https://publiclab.org/notes/cfastie/08-26-2014/new-ndvi-colormap>.
- [9] Janet Nichol. “A GIS-Based Approach to Microclimate Monitoring in Singapore’s High-Rise Housing Estates”. In: *Photogrammetric Engineering & Remote Sensing* 60 (Jan. 1994), pp. 1225–1232.
- [10] P. Ramamurthy and E. Bou-Zeid. “Heatwaves and urban heat islands: A comparative analysis of multiple cities”. en. In: *Journal of Geophysical Research: Atmospheres* 122.1 (2017), pp. 168–178. ISSN: 2169-8996. DOI: [10.1002/2016JD025357](https://doi.org/10.1002/2016JD025357). (Visited on 09/03/2023).
- [11] Prathap Ramamurthy et al. “Influence of Subfacet Heterogeneity and Material Properties on the Urban Surface Energy Budget”. EN. In: *Journal of Applied Meteorology and Climatology* 53.9 (Sept. 2014), pp. 2114–2129. ISSN: 1558-8424, 1558-8432. DOI: [10.1175/JAMC-D-13-0286.1.xml](https://journals.ametsoc.org/view/journals/apme/53/9/jamc-d-13-0286.1.xml) (visited on 09/03/2023).
- [12] D. A. Sachindra et al. “Impact of climate change on urban heat island effect and extreme temperatures: a case-study”. en. In: *Quarterly Journal of the Royal Meteorological Society* 142.694 (2016), pp. 172–186. ISSN: 1477-870X. DOI: [10.1002/qj.2642](https://doi.org/10.1002/qj.2642). (Visited on 09/16/2023).
- [13] M. Santamouris. “Recent progress on urban overheating and heat island research. Integrated assessment of the energy, environmental, vulnerability and health impact. Synergies with the global climate change”. In: *Energy and Buildings* 207 (Jan. 2020), p. 109482. ISSN: 0378-7788. DOI: [10.1016/j.enbuild.2019.109482](https://doi.org/10.1016/j.enbuild.2019.109482). URL: <https://www.sciencedirect.com/science/article/pii/S0378778819326696> (visited on 10/08/2023).
- [14] Michael Schultz et al. “Open land cover from OpenStreetMap and remote sensing”. en. In: *International Journal of Applied Earth Observation and Geoinformation* 63 (Dec. 2017), pp. 206–213. ISSN: 15698432. DOI: [10.1016/j.jag.2017.07.014](https://doi.org/10.1016/j.jag.2017.07.014). URL: <https://linkinghub.elsevier.com/retrieve/pii/S0303243417301605> (visited on 09/24/2023).
- [15] José A. Sobrino, Juan C. Jiménez-Muñoz, and Leonardo Paolini. “Land surface temperature retrieval from LANDSAT TM 5”. In: *Remote Sensing of Environment* 90.4 (Apr. 2004), pp. 434–440. ISSN: 0034-4257. DOI: [10.1016/j.rse.2004.02.003](https://doi.org/10.1016/j.rse.2004.02.003). URL: <https://www.sciencedirect.com/science/article/pii/S0034425704000574> (visited on 09/20/2023).

- [16] I. D. Stewart. “A systematic review and scientific critique of methodology in modern urban heat island literature”. en. In: *International Journal of Climatology* 31.2 (2011), pp. 200–217. ISSN: 1097-0088. DOI: [10.1002/joc.2141](https://doi.org/10.1002/joc.2141). URL: <https://onlinelibrary.wiley.com/doi/abs/10.1002/joc.2141> (visited on 10/08/2023).
- [17] U.S. Environmental Protection Agency (EPA). “Reducing urban heat islands: Compendium of strategies”. In: (2008). URL: <https://www.epa.gov/heatislands/heat-island-compendium>.
- [18] USGS. “Landsat 7”. In: (). URL: <https://www.usgs.gov/landsat-missions/landsat-7>.
- [19] USGS. “Landsat 8”. In: (). URL: <https://www.usgs.gov/landsat-missions/landsat-8>.
- [20] *Using Landsat Level 1 Data Products*. URL: <https://www.usgs.gov/landsat-missions/using-usgs-landsat-level-1-data-product>.
- [21] Qihao Weng. “Fractal Analysis of Satellite-Detected Urban Heat Island Effect”. In: *Photogrammetric Engineering & Remote Sensing* 69.5 (May 2003), pp. 555–566. DOI: [10.14358/pers.69.5.555](https://doi.org/10.14358/pers.69.5.555).
- [22] Qihao Weng, Dengsheng Lu, and Jacquelyn Schubring. “Estimation of land surface temperature–vegetation abundance relationship for urban heat island studies”. en. In: *Remote Sensing of Environment* 89.4 (Feb. 2004), pp. 467–483. ISSN: 0034-4257. DOI: [10.1016/j.rse.2003.11.005](https://doi.org/10.1016/j.rse.2003.11.005). URL: <https://www.sciencedirect.com/science/article/pii/S0034425703003390> (visited on 01/15/2023).
- [23] Robert L Wilby. “Constructing Climate Change Scenarios of Urban Heat Island Intensity and Air Quality”. en. In: *Environment and Planning B: Planning and Design* 35.5 (Oct. 2008), pp. 902–919. ISSN: 0265-8135. DOI: [10.1068/b33066t](https://doi.org/10.1068/b33066t). (Visited on 09/16/2023).